Numerical simulation of the plunge stage in friction stir welding - different tools

H. Dascau[1], A. Sedmak[2], M. Rakin[3], D. Veljic[4], M. Perovic[5], B.Medjo[3] and N. Bajic[4]

[1]National R&D Institute for Welding and Material Testing, Timisoara, Romania
[2]Faculty of Mechanical Engineering University of Belgrade, Serbia
[3]Faculty of Technology and Metallurgy University of Belgrade, Serbia
[4]IHIS Science & Technology Park Zemun, Belgrade, Serbia
[5]Chamber of Economy of Montenegro, Podgorica, Montenegro

E-mail: dascau@isim.ro

Keywords

Friction stir welding, conical shoulder, flat shoulder, numerical simulation, temperature fields

1. Introduction

Friction stir welding has two different stages including a plunge and a linear welding phase as shown in Figure 1. In the plunge stage, a FSW tool penetrates the workpieces to be welded. In the linear welding phase, the tool moves along

(a) Plunge stage (b) Welding stage

Figure 1. Friction stir welding process [1]

the joint line. The whole process adds frictional heat with intense plastic deformation to generate joints and the plunge stage of FSW process is crucial since most of the

Table 1. Material properties of AA5083-H116 [2]

Material properties	Value
Young's Modulus of Elastic. (GPa)	71
Poisson's Ratio	0.33
Tensile Yield Strength (MPa)	228
Ultimate Tensile Strength (MPa)	317
Thermal Conductivity (W/mK)	117
Coefficient of Thermal Expansion (°C $^{-1}$)	23.8×10^{-6}
Density (kg/m^3)	2660
Specific Heat Capacity (J/Kg °C)	900

thermomechanical conditions are initiated and the highest temperature and forces are required in this stage during the whole process. This paper investigates the plunge stage using three-dimensional finite element mode and two different tools.

2. Material properties

In the present work, material of the welding plate is AA5083-H116. Chemical composition of AA5083-H116 aluminium: Aluminium (Al) - Balance, Cu - 0.1, Mg - 4.5, Mn - 0.65, Fe - 0.3, Si - 0.12, Zn - 0.09, Ti - 0.15, Cr - 0.1, other, total - 0.02 % [2]. The thermal and mechanical properties used in this model are given in Table 1. The material of the tool is steel 155CrVMo121. The material of the backing plate is steel 42CrMo4.

3. Model Description

Geometry and finite element mesh

The model consists of a deformable workpiece, a rigid stir welding tool and a rigid backing plate. The welding plate in the numerical model is dimension 50 x 50mm and 6mm in

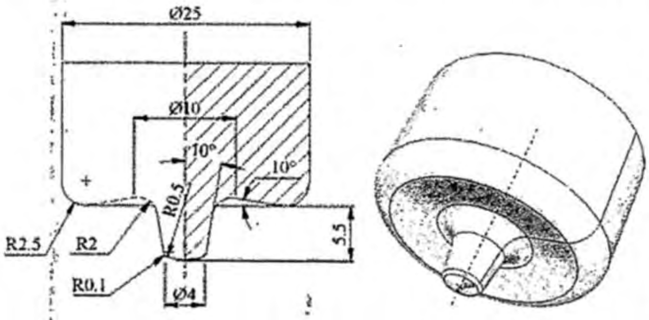

Figure 2. A conical shoulder tool with angle of 10°

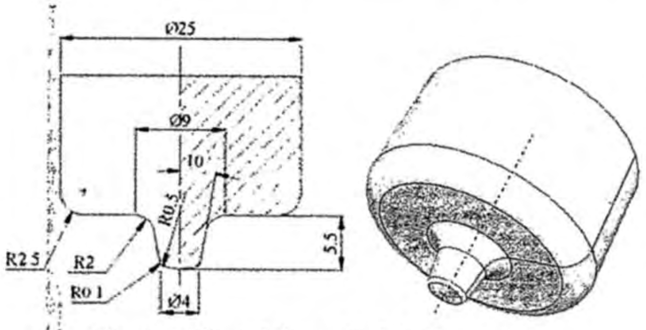

Figure 3. The welding tool with a flat shoulder

thickness. For three-dimensional numerical model used is C3D8RT element type which is a thermo-mechanically coupled hexahedral element with 8-nodes each having trilinear displacement and temperature degrees of freedom. This element produces uniform strain (first-order reduced integration) and contains hourglass control [3]. The mesh consists of 27,900 nodes and 25,166 elements.

The tool and the backing plate is modelled as a rigid surface having no thermal degrees of freedom. The main tool geometry in the FE model is similar to the experimental tool. This numerical simulation of the plunge stage in friction stir

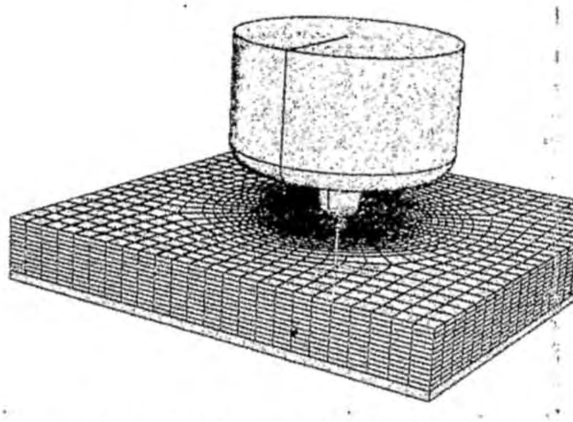

Figure 4. The numerical model of welding plate, tool and backing plate

welding using two different tools. The first tool have a conical shoulder with angle of 10° - Figure 2 and the second tool have a flat shoulder - Figure 3. The numerical model of welding plate, tool and backing plate is shown in Figure 4.

Johnson-Cook elastic-plastic model

In order to avoid the unacceptable mesh distortion caused by the large deformation process, a thermo-mechanical finite element model based on the arbitrary Lagrangian-Eulerian formulations and the adaptive meshing were employed in this study. Adaptive meshing in ABAQUS/Explicit [4] combines features of Lagrangian and Eulerian analyses and is referred to as an ALE analysis. The selection of an appropriate constitutive law to reflect the interaction of flow stress with temperature, plastic strain and strain rate is essential for modelling the FSW process. For this reason the temperature and strain rate-dependent elastic-plastic Johnson-Cook law is selected for this model [5]. The contact forces in the normal direction of the surfaces are modelled by Coulomb's Law of friction. The elastic-plastic Johnson-Cook material law is given by (It is available in ABAQUS finite element code) [4], [6]:

$$\sigma_y = \left[A + B(\varepsilon_p)^n\right]\left[1 + C\left(\frac{\dot{\varepsilon}_p}{\dot{\varepsilon}_o}\right)\right]\left(1 - \left(\frac{T - T_{room}}{T_{melt} - T_{room}}\right)^m\right) \quad (1)$$

where is T_{melt} = 620 °C the melting point or solidus temperature, T_{room} = 20 °C the ambient temperature, T (°C) the effective temperature, A=167 MPa the yield stress, B = 596 MPa the strain factor, n = 0.551 the strain exponent, m=0.859 the temperature exponent, C=0.001 the strain rate factor. A, B, C, n, T_{melt}, T_{room} and m are material/test constants for the Johnson-Cook strain rate dependent yield stress for AA5083-H116 [7].

Thermal model

The heat generation in the friction stir welding is assumed to be a combination of two different mechanisms: (1) the friction at the tool and work piece interfaces, and (2) the plastic shear deformation of the weld metal in the vicinity of the pin. The heat produced during welding is dissipated via conduction into the work piece, the tool and the backing plate as well as via convection and radiation from the work piece surfaces. The heat loss due to radiation is presumably negligible because of the low temperatures involved with the process and can be combined with the convective heat transfer from the top surface of the plate to the ambient by utilizing a slightly elevated heat transfer coefficient [6]. The governing equation for heat transfer process during the plunge phase of FSW process can be written as:

$$\rho c\frac{\partial T}{\partial t} = \frac{\partial}{\partial x}\left[k_x\frac{\partial T}{\partial x}\right] + \frac{\partial}{\partial y}\left[k_y\frac{\partial T}{\partial y}\right] + \frac{\partial}{\partial z}\left[k_z\frac{\partial T}{\partial z}\right] + \dot{q}_p \quad (2)$$

where ρ is the density, c is the specific heat, k is heat conductivity, T is the temperature, t is the time, $\dot{q}_p$ is heat generation coming from plastic energy dissipation due to shear deformation, and x, y, and z are spatial coordinate [8]. The rate of heat generation due to plastic energy dissipation, $\dot{q}_p$ is computed from

$$\dot{q}_p = \eta\sigma\dot{\varepsilon}^{pl} \quad (3)$$

where η is the factor of converting mechanical to thermal energy (0.9) [9], σ is the shear stress, and $\dot{\varepsilon}^{pl}$ is the rate of plastic strain.

Heat generation of frictional heating between tool and workpieces can be written as:

$$\dot{q}_f = \frac{4}{3}\pi^2\mu PNR^3 \quad (4)$$

where $\dot{q}_f$ is the frictional heat generation, μ is the coefficient of friction, P is the traction, N is the rotational speed and R is the surface radius.

4. Results and discussion

A coupled thermo-mechanical model was developed to study the temperature fields of alloy AA5083-H116 under rotating speed of 400 r/min, during the plunge stage in friction stir welding (FSW) process. Here is used tool with a flat shoulder and tool with a conical shoulder. The heat transfer through the bottom surface of the workpiece is controlled by the heat transfer coefficient of 1000 W/m^2K. A constant friction coefficient of 0.3 is assumed between the tool and the workpiece and the penalty contact method is used to model the contact interaction between the two surfaces. Heat convection coefficients on the surface of the workpiece are h = 10 W/m^2K with the ambient temperature of 200°C [9].

Figure 5 and 6 shows the temperature fields in the transverse cross section near the tool/matrix interface after 28.5 s. This transient temperature field is symmetric. The maximum temperature is lower than the melting point of the welding material (T_{melt} = 620°C). The welding temperature created by FSW ranges from 80 to 90% of the melting temperature of the welding material.

Tools have a different shoulder and same a pin. At the start of FSW, during plunging of the pin, until the moment of contact between tool shoulder and the welding plate, the heat generated is same for both tools. Tool with a flat shoulder is the first made contact between shoulder and the welding plate. This is longer the time of friction between the tool

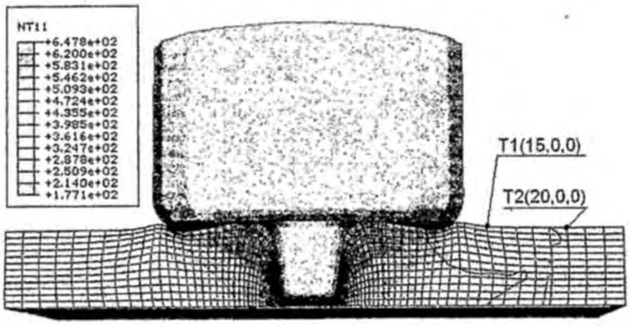

Figure 5. The temperature fields in the transverse cross section near the tool/matrix interface after 28.5 s, when rotation speeds is 400 r/min and a conical shoulder tool with angle of 10°.

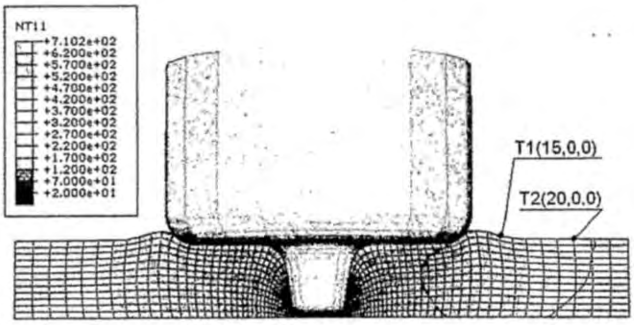

Figure 6. The temperature fields in the transverse cross section near the tool/matrix interface after 28.5 s, when rotation speeds is 400 r/min and a flat shoulder tool.

shoulder and welding plate which results in more heat generated. This applies to the plunge stage. In the linear welding phase, using tool with a conical shoulder, which results in more heat generated, because the larger contact area between the tool shoulder and welding plate[10].

Figure 7 and 8 shows typical temperature distribution over one-half of the workpiece obtained by cutting along transverse directions. It's the temperature field of the plunge stage after 28.5 s when rotation speeds is 400 r/min. The

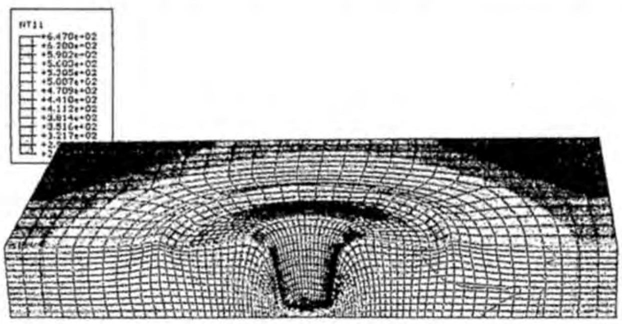

Figure 7.Temperature distribution in aluminium AA5083-H116 at the end of a 28.5 s plunge. A conical shoulder tool with angle of 10°.

plunge depth is 5.7 mm. The tool plunge velocity is set to a uniform value of 0.2 mm/s. This temperature field is symmetric. The concavity is designed to provide a reservoir of material above the original crown surface of the weld, facilitate transport of material around the tool and reduce plate thinning in the weld zone. The plasticised material is extruded from the leading to the trailing side of the tool but is trapped by the

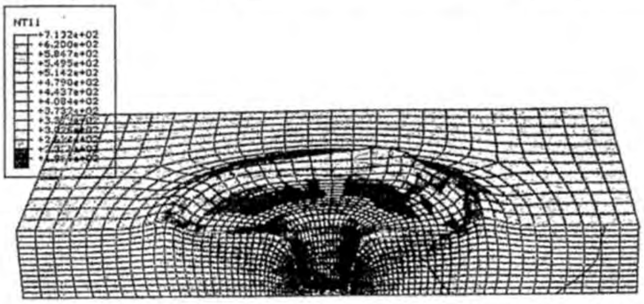

Figure 8. Temperature distribution in aluminum AA5083-H116 at the end of a 28.5 s plunge. The welding tool with a flat shoulder.

conical shoulder which moves along the weld to produce a smooth surface finish. On the advancing side of the crown of the weld, a lip forms where weld metal is rolled over onto the base metal. This lip is often called "flash" and can be minimized, but not eliminated, by a proper choice of welding parameters and tool design - using tool with a conical shoulder [11].

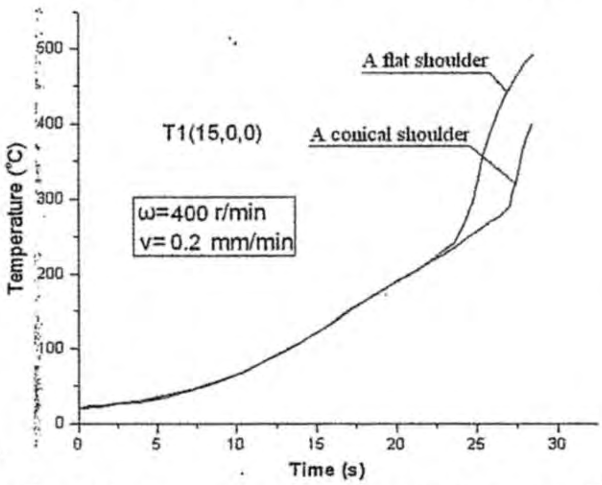

Figure 9. The temperature dependence of the time (point T1)

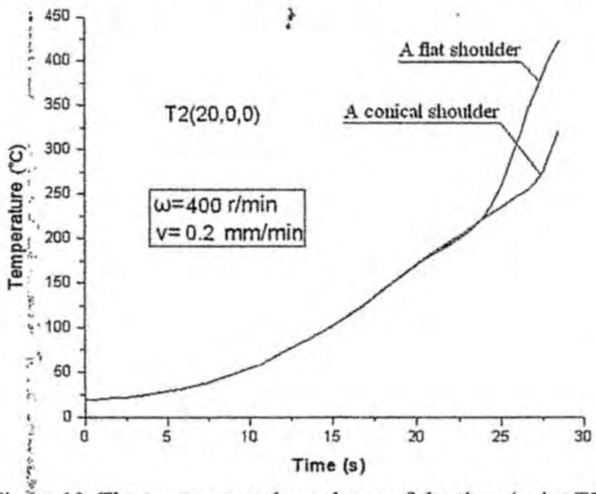

Figure 10. The temperature dependence of the time (point T2)

Figure 9 and 10 shows the temperature dependence of the time for plunge stage, when rotation speeds is 400 r/min in the points T1 (15, 0, 0) and T2 (20, 0, 0). Numerical results indicate that the maximum temperatures of the plunge stage in friction stir welding are higher by using tool with a flat shoulder than by using tool with a conical shoulder for the same rotation speed.

5. Conclusions

The temperature in the matrix is lower than the melting temperature.

The temperature field is symmetric.

The concavity is designed to provide a reservoir of material above the original crown surface of the weld, facilitate transport of material around the tool and reduce plate thinning in the weld zone.

The "flash" can be minimized, but not eliminated, by a proper choice of welding parameters and tool design - using tool with a conical shoulder.

The maximum temperatures of the plunge stage in friction stir welding are higher by using tool with a flat shoulder than by using tool with a conical shoulder for the same rotation speed.

References

[1]. Mahoney, M.W., Mishra, R., Nelson, T.: High Strain Rate Superplasticity in Thick Section 7050 Aluminium Created by Friction Stir Processing, Proceedings of the Third International Symposium on Friction Stir Welding, Kobe Exhibition Centre, Port Island, Kobe, Japan, September 2001 (distributed by TWI on CD)

[2]. xxx: http://asm.matweb.com/search/SpecificMaterial.asp?bassnum=MA5083H116

[3]. Zhang, Z., Bie, J., Zhang, H.: Effect of Traverse/Rotational Speed on Material Deformations and Temperature Distributions, Friction Stir Welding. J. Mater. Sci. Technol. 24 (2008) 907-913

[4]. xxx: Abaqus Inc., Analysis - User's Manual v.6.7, 2007

[5]. Mandal, S., Rice, J., Elmustafa, A.A.: Experimental and numerical investigation of the plunge stage in friction stir welding, Journal of Materials Processing Ttechnology 203 (2008) 411-419

[6]. Veljic, D., Perovic, M., Medjo, B., Rakin, M., Sedmak, A., Dascau, H.: Thermo-mechanical modelling of Friction Stir Welding, The 4th International Conference, Innovative technologies for joining advanced materials, June 10 - 11, 2010., Zbornik radova, str. 171-176, CD

[7]. xxx: http://www.journalamme.org/papers_vol37_2/37248.pdf

[8]. xxx: Kwanghyun Park, Development and analysis of ultrasonic assisted friction stir welding process, Doctor of Philosophy (Mechanical Engineering) in The University of Michigan, 2009

[9]. Schmidt, H., Hattel, J.: A local model for the thermomechanical conditions in friction stir welding. Modelling Simul. Mater. Sci. Eng. 13 (2005) 77-93

[10]. Mishra, R., Murray, W., Mahoney, M.W.: Friction stir welding and processing, http://books.google.com

[11]. Veljic, D.: Technology of Friction Stir Welding of Aluminium Alloys. M.Sc. Thesis, Faculty of Mechanical Engineering, University of Belgrade

Lecture presented at the 5th International Conference "Innovative Technologies for Joining Advanced Materials", Timisoara - Romania (June 16-17, 2011)